16th World Conference on Earthquake Engineering, 16WCEE 2017
Santiago Chile, January 9th to 13th 2017
Paper N° 2285
Registration Code: S-W1466343194

DESIGNING FOR DAMAGE ACCUMULATION AND LOW CYCLIC FATIGUE IN REINFORCED CONCRETE BRIDGE COLUMNS

O. Lara(1), D. Toro(2), C. Ventura(3)

(1) Professor, University of Guayaquil, Ecuador, ottonlara@hotmail.com
(2) Assistant Professor, Escuela Superior Politécnica del Litoral. danieltorocastillo@yahoo.com
32) Professor, University of British Columbia, ventura@civil.ubc.ca

Abstract

Two columns tested in shake table under several records suffered damage for the design earthquake and the damage increased after the following records. To predict the test results, a damage accumulation (DA) and a low cyclic fatigue (LCF) models, both based on strain responses, were incorporated to a fiber finite element model (FFEM2) demonstrating 1) that FFEM2 results were close to test measures, 2) that to meet performance based seismic design it is convenient to accumulate the damage induced by each record and remove the fibers that reached 100% DA by means of the LCF model. When DA and LCF models are not included in FFEM2, the major damages to be prevented, observed during tests, are not predicted. A practical solution to prevent failures by LCF, based on increasing the confinement of the concrete, is proposed.

Keywords: damage accumulation, low cyclic fatigue, bridge columns

1. Introduction

Materials have memory and a fatigue life, and reversal strains, capable to induce vertical cracks in the cover or initial yielding in the steel, start a damage accumulation (DA) process which increases during the strong duration of the motion reducing the fatigue life of the materials. If more earthquakes excite the column, DA will increase more and the fatigue life of the materials may be exhausted causing failure by Low Cyclic Fatigue (LCF), a physical phenomenon that occurs when DA reaches 100%.

The use of one earthquake per performance level for retrofit design is recommended in [1] and [2, 3] to meet Performance Based Seismic Design (PBSD) however, there is no prescription to accumulate the effects of each earthquake, a necessary procedure for design of long life-time structures, as bridges.

The study focuses on the calculation of DA and LCF and its effects in bridge columns using finite fiber element models (FFEM) [4] and FFEM2, developed in this study. Both are based on the OpenSees framework (Open System for earthquake engineering simulation) that is an Object-oriented Finite Element Program [5, 6].

Two columns, tested in shake table under several records, are studied using FFEM2 to simulate the responses of the materials. Lara [4], using FFEM, predicted the fracture of bars due to LCF in one of the columns and the response of the other using FFEM2, deserving a prize of excellence [7].

2. Objectives and Scope

Objectives. 1) To study strain response when previous records effects (PRE) are captured and when such effects are not captured (NPRE), 2) If both responses are different, verify if the damages are due to DA and LCF using FFEM2 to predict the damages observed during the tests after each record, and 3) If DA and LCF caused the damage, to suggest simple solutions for design of bridge columns.

Scope. The columns, shake table tested, one in UC San Diego (UCSD) [8] and the other, in UC Berkeley (UCB) [9], are studied only for flexural response because columns were designed preventing shear failure. Responses are captured in only in one direction, as they were tested.

3. The Fiber Finite Element Model 2 (FFEM2)

3.1 Description of the model

Fig. 1(a) shows the 3-D Finite Fiber Element Model (FFEM2) [4] which contains three beam-column elements, [10], and Fig. 1(b) the section of the column, located at the ends of each element. The initial model, FFEM, required calibration of several parameters [4]: lengths of plastic hinge (L_p) and strain penetration (L_{sp}) which are similar to equations in [13], inelastic parameters for steel bars [12]: R_0= 20, R_1 = 0.925, and R_2 = 0.15, and damping ratio ξ = 0.03. The constitutive relations for the concrete [11] and the steel [12], are explained in [4].

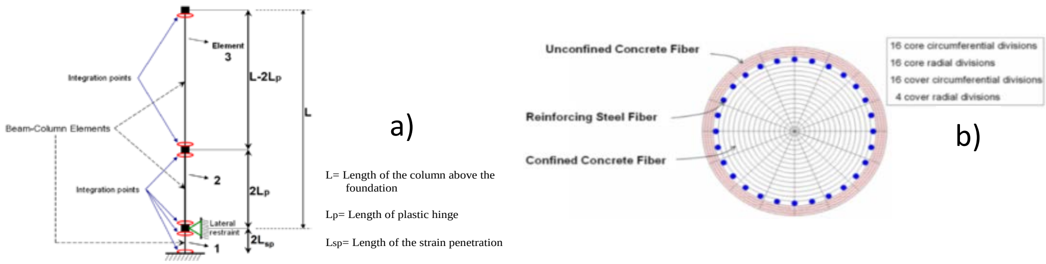

Fig. 1 (a) – 3-D Finite Fiber Element Model 2, FFEM2; (b) – section of the bridge column

FFEM2 developed in this study is based on FFEM, and includes: 1) DA and LCF models for the concrete, and 2) a compression Gap in the concrete fibers connected in series to the plastic hinge element. The Gap eliminates tension strains not existing in the concrete material model [4].

4. DA and LCF models for UC San Diego (UCSD) and UC Berkeley (UCB) columns

4.1 DA and LCF models included in FFEM2.

DA model [14] calculates the increasing damage induced by strain reversals in the materials, and LCF model [15, 16] controls the number of cycles at different strain amplitudes ε_i inducing failure Eq. (1), and removes the fibers reaching 100% DA. In this study, materials damages are cracking, spalling, and yielding, and associated failures, as specified in the code, are: crushing of the core, which starts close to the bars and grows inside the column, fracture of bars, and instability.

$$\varepsilon_i = \varepsilon_0 [N_{fi}]^{-m} \tag{1}$$

ε_i = strain amplitude response captured by FFEM2, ε_0 = strain at which the material fails in one cycle, N_{fi} = the number of accumulated cycles with amplitude ε_i inducing failure by LCF, m = slope of the line of failure

The equation for the steel in UCSD column bars after calibration of ε_0 and m [4], for $\varepsilon_s \geq 0,0026$ is:

$$\varepsilon_i = 0.07 [N_{fi}]^{-0.37} \tag{2}$$

For the concrete, calibrations of ε_0 are: for spalling ε_0 = 0.006 (UCSD (2010)), and for crushing of the core, from [11], ε_0 = 0.02. Calibration of m is explained below.

The damage induced by each strain is calculated using Eq. (3) [14]:

$$D_i = n_i / N_{fi} \tag{3}$$

n_i is the number of strains with amplitude ε_i captured in each strain history response, and DA ([14] is:

$$DA = \Sigma D_i \tag{4}$$

To calculate D_i, one unknown: m, still needs definition and there are not fatigue tests on reinforced concrete columns that could support calibrations therefore, to calibrate an iterative procedure was performed:

From the history response assume m and for each strain reversal ε_i larger than 0.0015 [20], calculate N_{fi} Eq. (1). D_i induced by each strain is calculated with Eq. (5) and DA with Eq. (4). DA should be equal to unity at the time of failure, if not, start iterations changing m until DA = 1.0 at failure. The procedure permits to calculate the number of cycles with amplitude ε_i to induce LCF and to build the line of failure.

$$D_i = 1/N_{fi} \tag{5}$$

After several iterations, the fatigue equations for LCF in the concrete, in the UCSD column, are:

In the unconfined concrete: $\varepsilon_i = 0.006[N_{fi}]^{-0.63}$ (6)

In the confined concrete, West side: $\varepsilon_i = 0.02[N_{fi}]^{-0.76}$ (7)

In the confined concrete, East Side: $\varepsilon_i = 0.02[N_{fi}]^{-0.89}$ (8)

The procedure used for UCSD column is also used for UCB column. The parameters for the cover are similar in both columns, but ε_0 for the core vary due to [11] and there are slight differences in m. ε_0 and m also vary for the steel in UCB column, Eq. (12), due to the differences in the diameter of the bars, [4],[17].

In the unconfined concrete: $\varepsilon_i = 0.006[N_{fi}]^{-0.63}$ (9)

In the confined concrete, West side: $\varepsilon_i = 0.015[N_{fi}]^{-0.84}$ (10)

In the confined concrete, East side $\varepsilon_i = 0.015[N_{fi}]^{-0.77}$ (11)

In the steel bars: $\varepsilon_i = 0.16[N_{fi}]^{-0.57}$ (12)

These equations deliver an equivalent N_{fi} for a constant strain but, fatigue means a number of strains of different amplitudes associated to the same N_{fi} causing DA or LCF therefore, the procedure to calibrate m secures the participation of the strains captured during responses.

5. The UCSD column and records used for the test and simulation

The reinforced concrete bridge column was tested under several earthquakes: frequent (EQ1), moderate (EQ2), occasional or design (EQ3), aftershock (EQ4), strong (EQ5), and aftershock (EQ6). Then, EQ7 was applied four times named EQ7 to EQ10 to induce the collapse, [18]. EQ7 is considered here as the rare earthquake. Table 1 shows the sequence of the records filtered by the shake table, and the Scale Factor (SF) for each one, and Fig. 2 shows the materials characteristics and design parameters of the column.

6. Limits for seismic design preventing failures: UCSD column

The code [19] specified limits are: 1) Ultimate confined concrete strain: $\varepsilon_{cu} \leq 0.02$, 2) Ultimate steel strain: $\varepsilon_{su} \leq 0.09$ for the 35mm bars, 3) Instability: $P\text{-}\Delta \leq 0.25M_p$, P = 2380kN and M_p = 5800kN-m Fig. 3(b), $\Delta = u_m$ = 60cm. 4) $\mu \leq 5$, $u_{max} = \mu u_y$. u_y = 10cm, $u_{max} \leq$ 50cm. A larger μ is not a failure then, u_m = 60cm, controls the design, Fig. 3.

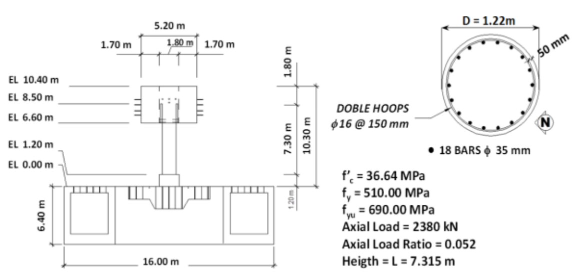

Fig. 2 - Geometry and material characteristics

Table 1 - Structure period, T, Scale factor (SF) x record, peak ground acceleration (PGA) / period (T_s) of the record.

T= Period (s)	EQ: SFxRecord	PGA / T record (s)	EQ: SFxRecord	PGA / T record (s)
T structure = 0.94s	EQ1: 1.0Agnews	0.20g / 0.10	EQ6: 1.0EQ3	0.50g / 0.65
	EQ2: 1.0Corralitos	0.40g / 0.10	EQ7: 1.0Takatori	0.71g / 1.31
	EQ3: 1.0Los Gatos	0.50g / 0.65	EQ8: -1.2EQ7	0.85g / 1.31
	EQ4: 1.0 EQ2	0.40g / 0.10	EQ9: 1.2EQ7	0.85g / 1.31
	EQ5: -0.8Takatori	0.57g / 1.31	EQ10: 1.2EQ7	0.85g / 1.31

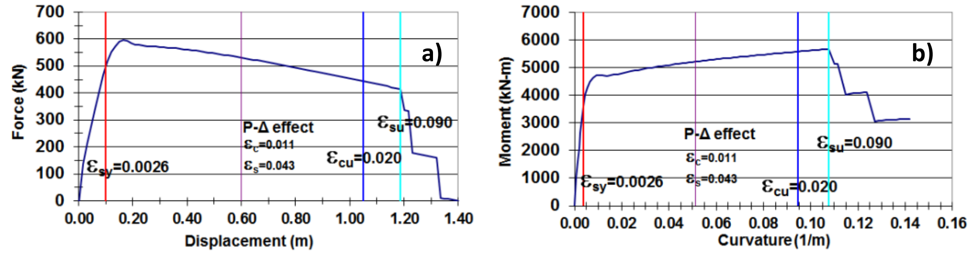

Fig. 3 - Lateral monotonic capacity of the column, (a) Force-Displacement and; (b) Moment-Curvature

7. Inelastic and fatigue study of the UCSD column to the ten records

7.1 Comparison of hysteretic responses: PRE and NPRE

Inelastic dynamic responses (IDR) including DA and LCF analysis are calculated simultaneously. This is the reason why DA is captured during IDR, called previous records effects (PRE) responses, while NPRE means no DA. PRE responses show, since EQ3, stiffness degradation due to both: spalling, which starts the DA process, and crushing and, since EQ8, reductions of strength and displacement capacities due to fracture of bars and crushing, while NPRE responses show only the effect of IDR to each record and there is no material failure.

PRE and NPRE responses to the less damaging earthquakes: EQ1 and EQ2, are similar since both responses are close to elastic. Fig. 4 shows PRE and NPRE responses for EQ7, when crushing starts close to the bars, and to EQ9, when bars fractured inducing loss of strength and stiffness.

7.2 Force-Displacement responses

Fig. 5 shows the force-displacement (F-D) responses of the column to a long pulse applied at the end of each earthquake, and Table 2 the stiffness for PRE and NPRE responses: KPRE and KNPRE, measured at a force of 100kN. K_0 is the initial stiffness measured in the F-D curve for EQ1 at the same force. Since EQ3 and on, KPRE is lower than KNPRE, also energy dissipation capacities, and drifts and ductility demands, Table 2. It is observed the reduction in strength at maximum displacement once bars fractured and crushing continued.

7.3 Concrete strain histories for PRE and NPRE responses

In this study, strains reversals equal or larger than 0.0015 [20] cause vertical cracks and DA leading to spalling of the cover and crushing of the confined concrete. In the bars DA starts at the yielding strain 0.0026 as it was tested in UCSD [8]. The history responses are in [21].

In Fig. 6, PRE responses show, from EQ2 to EQ7, 16 peaks in the West and 12 in the East larger than 0.0015 inducing DA which reached 100% at EQ7 and the core crushed. Since there is no DA for NPRE responses, there are only 2 peaks in the West and 2 in the East for EQ7, larger than the peaks recorded for PRE responses, but not enough in number to induce crushing.

DA depends on the number and amplitude of strains reversals captured during each record, therefore individual responses to earthquakes do not provide the appropriate information for seismic design and even worse if several records are used to meet PBSD.

In the following sections, results are related to crushing of the confined concrete since this failure, as captured by FFEM2 and coinciding with [8], occurred due to DA and LCF, before than instability and fracture of bars changing the code limits to prevent failures. Effects of DA and LCF on the steel bars is in [21]

7.4 Statistics of strain responses, PRE captured

The histograms and the percentage of damage calculated with Eq. (6), Eq. (7), and Eq. (8) per interval of strains, is shown in Fig. 7 for the West and East sides.

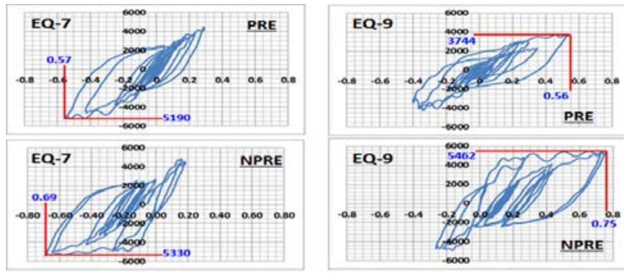

Fig. 4 - Hysteretic responses to records EQ7 and EQ9 PRE and NPRE

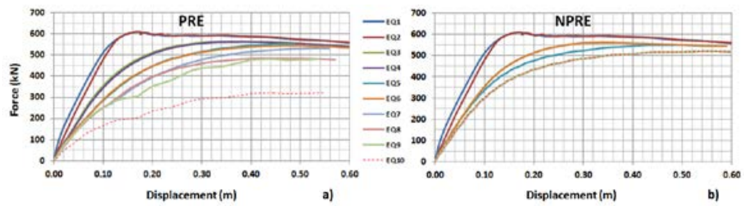

Fig. 5: Force-displacement curves. a) PRE, b) NPRE

Table 2 – PRE and NPRE responses

	PRE						NPRE					
EQ	Max. Displacement demand, u_{max} (cm)	Max. Strength demand, V_{max} (kN-m) at u_{max}	Total Energy dissipation capacity (kN-m-m)	K_{PRE}/K_o	Drifts	μ_{PRE}	Max. Displacement demand, u_{max} (cm)	Max. Strength demand, V_{max} (kN-m) at u_{max}	Total Energy dissipation capacity (kN-m-m)	K_{NPRE}/K_o	Drifts	μ_{NPRE}
EQ1	7	2513	10.90	1.00	0.010	0.70	7	2513	10.90	1.00	0.010	0.70
EQ2	12	4519	210.60	0.96	0.016	1.20	12	4519	210.60	0.96	0.016	1.20
EQ3	36	5041	2716.90	0.37	0.049	3.60	36	5041	2812.00	0.42	0.049	3.60
EQ4	16	2695	198.76	0.34	0.022	1.60	12	4519	210.60	0.96	0.016	1.20
EQ5	48	5114	4981.60	0.33	0.066	4.80	57	5282	5396.27	0.41	0.078	5.70
EQ6	36	4617	2722.40	0.33	0.049	3.60	36	5041	2812.00	0.42	0.049	3.60
EQ7	57	5190	6503.00	0.29	0.078	5.70	69	5330	7261.60	0.38	0.094	6.90
EQ8	58	5118	8144.20	0.29	0.079	5.80	75	5462	9218.30	0.34	0.103	7.50
EQ9	56	3744	5565.60	0.30	0.077	5.60	75	5462	9221.70	0.34	0.103	7.50
EQ10	56	2528	3507.80	0.19	0.077	5.60	77	5462	9221.70	0.34	0.105	7.70

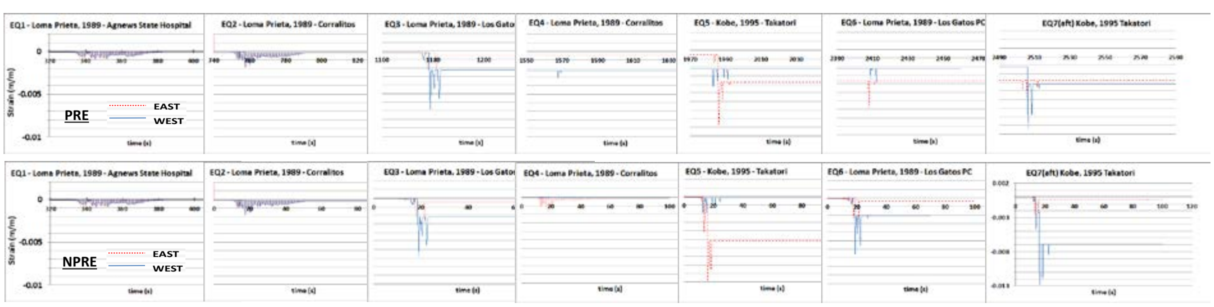

Fig. 6 - Strain histories for PRE and NPRE responses.

The displacement to prevent instability in this column is 60cm [19] however for PRE responses, crushing occurs during EQ7 at 57cm at ε_c = 0.0094 in the West after 16 strain reversals, and at ε_c = 0.0088 in the East after 12 reversals, while the code strain to prevent crushing is ε_{cu} = 0.02, no reversals included. These maximum strains captured at both sides, at failure, induced only 19% and 20% DA respectively Fig. (7). Therefore, such strains were not the direct cause of crushing. The maximum NPRE strain captured during EQ7 is 0.0128, less than 0.02, larger than 0.0094, but there is no crushing since 4 reversals are not enough, as seen later in Fig. 9.

Therefore, crushing is not due to just one large strain but due to the large one and also due to several previous strains damaging the materials.

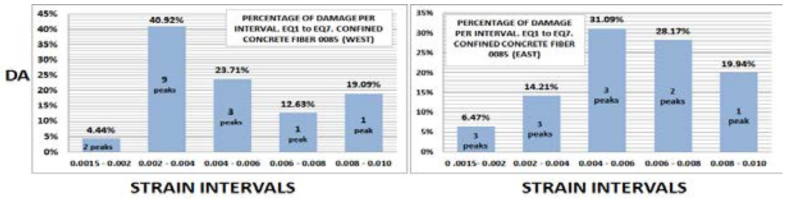

Fig. 7 - Percentages of damage per strain interval, West and East sides

Fig. 8 shows the state of the column, after EQ7, in the East side. Notice crushing of the concrete inside the hoops, enlargement of hoops, and bars starting to buckle.

Fig. 8 - State of the column after EQ7 (UCSD (2010))

8. Dynamic Fatigue Analysis (DFA) and design proposal to delay LCF

8.1 DA vs. time in the concrete and in the steel of the UCSD column: PRE and NPRE responses

Fig. 9 shows the relation DA vs. time, calculated using Eq. (6), Eq. (7), and Eq. (8) for the unconfined and confined concrete at the West and East sides of the UCSD column. It is observed in Fig. 9, that there is a progressive damage in the concrete: spalling and later crushing, both captured by FFEM2 in fibers 000 at the cover, and in fibers 0085, located 8.5cm inside the hoops, close to the bars.

In Fig. 9 the level of DA in the core, after full spalling during EQ5, is high, about 60% since the core cracked during EQ5 [8], therefore its potential to crush during EQ7 is also high. Fig. 12 shows that for NPRE responses, maximum DA in the core during EQ7 is 30% in the West because there is no DA captured.

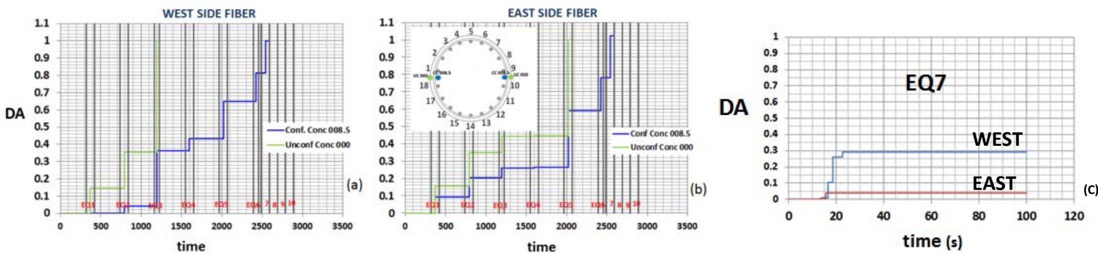

Fig. 9 - Variation of DA with time in the unconfined and confined concrete, (a) and (b): PRE responses, (c): NPRE response

The test report, [8], mentions that during EQ7, the confined concrete crushed at both sides, close to the bars, the hoops enlarged and they were not able to continue confining the core and supporting the bars so onset of buckling was observed. According to FFEM2, the fibers located 8.5cm inside the original perimeter crushed to the interior about 8cm at the column-foundation interface, decreasing with height up to about 75cm, in an inclined plane, Fig. 10.

During EQ8, 2 bars fractured and during EQ9, 4 more bars fractured. The bars started buckling during EQ7, but due to the large number of reversals strains, about 95, bars failed by LCF and not due to buckling [4], [22], Fig. 11. The fracture of bars due to DA requires a larger number of inelastic strains than peak compression strains to induce failures in the concrete.

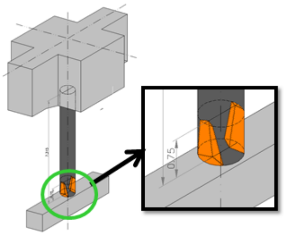

Fig. 10 - Crushing of the confined concrete

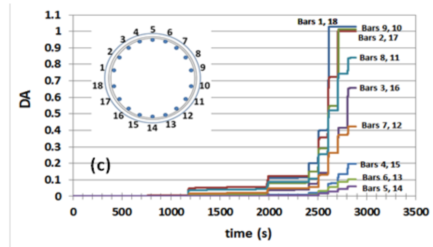

Fig. 11 - Variation of DA vs. time in the longitudinal steel bars

8.3 Designing to delay DA and LCF effects, UCSD column

DA and LCF effects demonstrated that failures in the concrete occur at reversals strain amplitudes lower than code limit strains therefore, following design philosophy proposed in [19], a possible solution to delay spalling and crushing due to LCF might be to increase the volumetric ratio of transversal reinforcement, improving the confined concrete constitutive relation [11].

The reduction in hoop spacing increases ε_{cu} [11] = ε_0 in Eq. (1), and also the number of peak compression strains required to reach crushing. After calibrations, if spacing is reduced from 15 to 9cm, using the same bar diameter, DA vs. time PRE results in Fig. 12 show that failure does not occur during the rare earthquake EQ7, but during EQ9 at both sides, therefore there is a delay in crushing. Also, the number of peak strains to crush the core, with the new spacing of the hoops, is 24 in the West and 18 in the East.

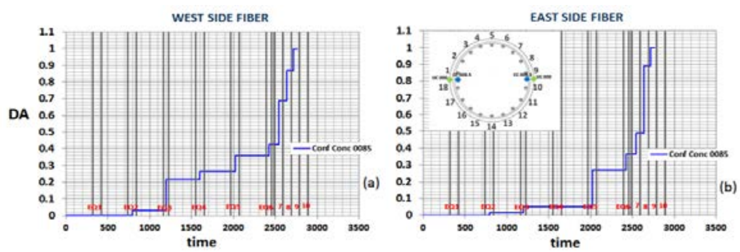

Fig. 12 - DA vs. time results in the confined concrete with the proposed new spacing of 9cm.

9. Column B1 tested at UC Berkeley (UCB)

9.1 Characteristics of the record and the column

In this study, UCB column [9] tested for one component of the Llolleo record, repeated several times with different scale factors (SF), is chosen to study the effects of DA and LCF. Table 3 shows the testing sequence.

Fig.13 shows the geometry of the prototype and the specimen, the longitudinal and transverse reinforcement, the properties of the materials, and the axial load. The Llolleo record applied to UCB column has a long duration close to two minutes and maximum PGA is 0.7g. The duration was reduced by 2.12 to shake the model and the record scaled up 1.29 times to reach the code spectrum for the design earthquake. The length scale prototype to model was 4.5 and the design of the column was performed using a strength reduction factor of 4.

Table 3 shows the characteristics of the record, the number of runs the record was applied to UCB column, the peak acceleration of the filtered records exciting the shake table during each run, and the damage observed after a run, [9].

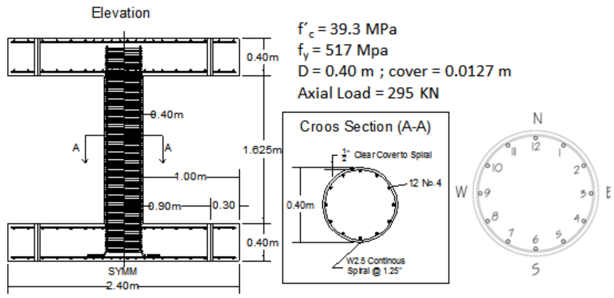

Fig. 13 - Geometry and material characteristics of UCB column [9]

Table 3 - Testing sequence, peak acceleration of the filtered records, and damage observed [9]

Run #	Performance Level	Table Displacement and Acceleration		Observations
		PGA[b] (g)	PGD[c] (in)	
		Long[b]	Long	
1	Low Level 1 13% Llolleo	0.03	0.19	No visible signs of damage.
2	Low Level 2 26% Llolleo	0.08	0.42	No visible signs of damage.
3	Yield Level 1 39% Llolleo	0.14	0.66	This level was slightly under yield. The observed displacement of the column was about 0.8 in. which is slightly less than the yield displacement of 1 in.
4	Yield Level 2 52% Llolleo	0.19	0.90	Slightly above yield. No visible damage.
5	Design Level 1 130% Llolleo	0.48	2.30	Some spalling occurred at the column base. Major flexural cracks were observed over a height of about 20 in. (1.25 D), with other cracks distributed over the height of the column.
6	Maximum Level 1 260% Llolleo	0.87	4.70	Spalled concrete fell off the base of the column. Bar #4 on the east side buckled and bars #2 and #3 were starting to buckle.
7	Design Level 2 130% Llolleo	0.46	2.32	Additional concrete damage due to this run was not significant. Smaller pieces of concrete were spalled. During each cycle, buckled bar #4 on the east side was pressing on the third spiral from the footing which was starting to kink at that location (observed in video replay).
8	Maximum Level 2 260% Llolleo	0.89	4.71	Two longitudinal bars and one spiral fractured. Bar #4 on the east-south side buckled more causing the spiral to fracture at that location. The middle longitudinal bar at the east side (#3) fractured in the tension part of the same cycle. The middle longitudinal bar at the west side (#9) fractured later in the run.
9	Maximum Level 3 260% Llolleo	0.91	4.73	On the west side, the north-west bar (#10) buckled, causing more crushing and fracturing a spiral. On the east side, the buckled bar (#4) fractured after losing confinement from the spiral which fractured in the previous run. The neighboring bar (#5) also buckled, extending the spalling well into the south face.

9.2 Strain and displacement code limits

In Fig. 14: 1) Ultimate confined concrete strain: $\varepsilon_{cu} \leq 0.015$, 2) Ultimate steel strain: $\varepsilon_{su} \leq 0.12$ for the 12.7 mm bars, 3) Instability: $P\text{-}\Delta \leq 0.25M_P$, since P = 290kN and M_P = 188kN-m Fig. 15, $\Delta = u_m$ = 16cm. 4) $\mu \leq 5$, $u_{max} = \mu u_y$. Since u_y = 3cm, $u_{max} \leq$ 15cm. A μ slightly larger than 5 is not a failure mechanism then, the limit displacement for the $P\text{-}\Delta$ effect, u_m = 16cm controls the design of the column.

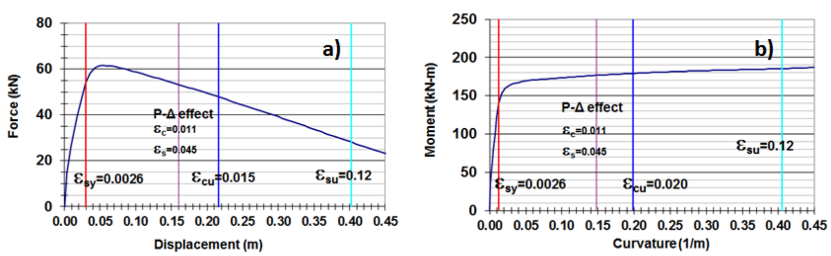

Fig. 14 - Lateral monotonic capacity of the column, (a) Force-Displacement and; (b) Moment-Curvature

10. Inelastic and fatigue study of the UCB column to the nine records

10.1 Comparison of results hysteretic responses: PRE and NPRE

Runs 1 and 2 are less than 27% Llolleo therefore, the hysteretic responses show slight changes in stiffness for PRE responses. However, DA causes stiffness degradation after Run 3, 39% Llolleo, and such reduction increases for Runs 4 and 5, 52% and 130% Llolleo, respectively. Runs 6, 8 and 9 contain the maximum design level: 2.6 Lolleo and Fig. 15 shows the hysteretic PRE and NPRE responses to Run 6, when crushing of the core occurred, and to Run 9 when 1 bar fractured, after fracture of 2 bars during Run 8. NPRE responses show less reductions in stiffness and strength than PRE responses.

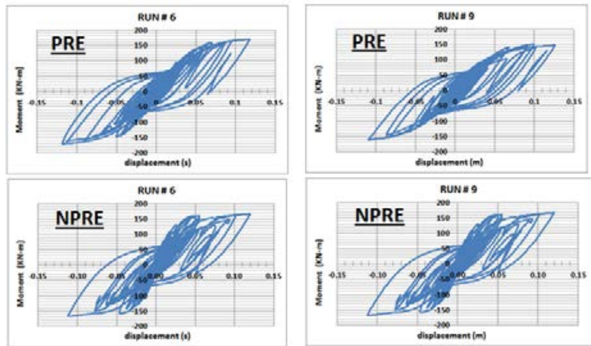

Fig. 15 - Hysteretic PRE and NPRE responses of UCB column

10.2 Force-Displacement responses

Fig. 16 shows the force displacement (F-D) responses of the column for the 9 Runs and for PRE and NPRE responses. As in UCSD column analysis, NPRE responses for UCB column exhibit larger stiffness, strength, drifts, and ductility ratio capacity because there is no DA captured, Table 4.

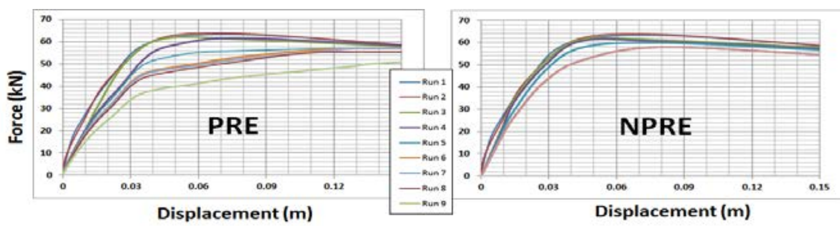

Fig. 16 – Force-Displacement responses of UCB column

Table 4 – PRE and NPRE responses of UCB column

	PRE						NPRE					
EQ	Max. Displacement demand, u_{max} (cm)	Max. Strength demand, V_{max} (kN) at u_{max}	Total Energy dissipation capacity (kN-m-m)	K_{PRE}/K_o	Drifts	μ_{PRE}	Max. Displacement demand, u_{max} (cm)	Max. Strength demand, V_{max} (kN) at u_{max}	Total Energy dissipation capacity (kN-m-m)	K_{NPRE}/K_o	Drifts	μ_{NPRE}
RUN # 1	1	27.8	1.55	1.00	0.004	0.330	1	27.8	1.55	1.00	0.004	0.330
RUN # 2	2.1	48.4	1.96	0.85	0.009	0.700	2.1	48.4	1.96	0.95	0.009	0.700
RUN # 3	2.9	58.9	2.36	0.45	0.012	0.970	2.9	58.9	2.36	0.55	0.012	0.967
RUN # 4	4.1	63.2	3.75	0.43	0.017	1.370	4.1	63.2	4.03	0.50	0.017	1.367
RUN # 5	7.1	66.3	29.70	0.38	0.029	2.370	8	67.0	34.85	0.45	0.033	2.667
RUN # 6	11.7	70.1	108.10	0.36	0.048	3.900	12	68.8	108.20	0.39	0.049	4.000
RUN # 7	7.1	60.4	26.29	0.34	0.029	2.370	8	67.0	34.85	0.45	0.033	2.667
RUN # 8	12.1	68.8	102.82	0.31	0.050	4.030	12	68.8	108.20	0.39	0.049	4.000
RUN # 9	12.6	66.0	101.10	0.26	0.052	4.200	12	68.8	108.20	0.39	0.049	4.000

10.3 Concrete strain histories for PRE and NPRE responses

In Fig. 17, PRE responses show in the concrete, from Run 4 to Run 6, 15 peaks in the West and 16 in the East larger than 0.0015 inducing DA which reached 100% at Run 6 when it is assumed here that the core crushed since 1 bar buckle and 2 others started to buckle, Table 3. NPRE response for Run 6 shows 7 peaks in the West and 8 in the East, however the number of reversals are not enough to induce crushing as it will be seen later.

As it was established for the UCSD column, PRE responses show that failures are related to the number and amplitude of the strains reversals (LCF), while NPRE results do not provide the appropriate information for seismic design, particularly if several records are used to meet PBSD.

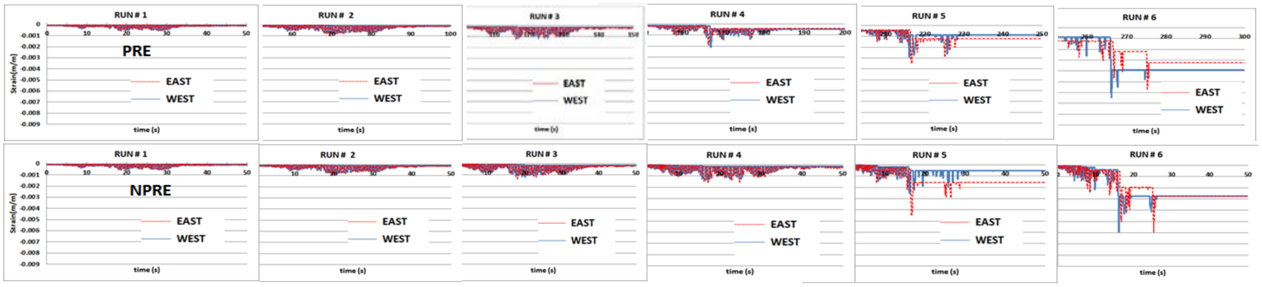

Fig. 17 - Strain histories for PRE and NPRE responses of UCB column

10.4 Statistics of strain responses, PRE captured

Statistics for the UCB column resemble those of the UCSD column. The strain at crushing [11] is ε_{cu} = 0.015 however, 1) the maximum strains and number of peaks in the West and East sides, PRE captured, are ε_c = 0.0064 and 15 peaks, and ε_c = 0.0058 and 16 peaks, causing 16% and 18% DA respectively at crushing at each side, 2) The reversals captured up to Run 6 are less than 0.015, but induced 100% DA and the core crushed close to the bars at both sides, 3) the maximum NPRE reversal captured during Run 6 is 0.006, at both sides, less than 0.015, but there was not crushing as it will be seen in Fig. 18.

Therefore, once again, crushing, a failure mechanism [19], is due to DA induced by several previous strains and not due to just the maximum captured at failure.

11. Dynamic fatigue analysis (DFA) and design proposal to delay LCF

11.1 Variation of DA vs. time in the confined concrete and in the steel bars, UCB column

Fig. 18 shows that there is no damage in the core for the first 3 runs, but for Run 4, when yielding occurred, DA in the core reached 4% at both sides. For run 5, the cover spalled and DA in the core is 32% in the West and 40% in the East. Crushing occurred at both sides, Run 6, and maximum displacement was 11.7cm. During NPRE response to EQ6, Fig. 18(c), DA reaches 24% in the West and 43% in the East therefore, there is no crushing because there is no DA measured for the previous records.

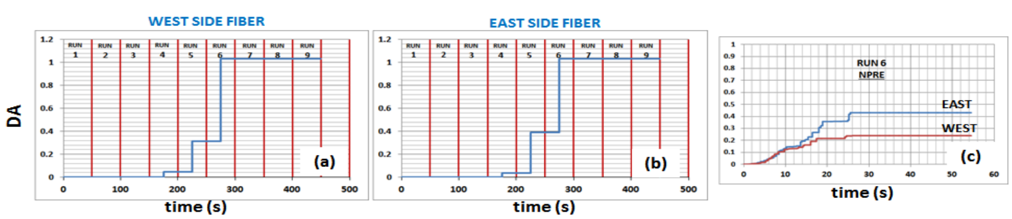

Fig. 18 –DA vs. time for confined concrete of UCB column

In the study about DA in the bars [4] Fig. 19, during Run 8 2 bars fractured and during Run 9, 1 more bar fractured, due to LCF in both cases. The bars started buckling during Run 6, but due to the large number of reversals strains, about 95, bars failed by LCF and not due to buckling [4], [22]. The fracture of bars requires a larger number of inelastic strains than peak compression strains required to induce failures in the concrete.

11.3 Delay DA and LCF effects, UCB column

Using the same procedure to delay effects of DA and LCF in the UCSD column, calibrations to increase the volumetric ratio of transversal reinforcement, to improve the confined concrete constitutive relation [11], show that for the UCB column if the spacing is reduced from 3.1cm to 1.8cm, same bar diameter, crushing is delayed to Run 9, Fig. 20. The number of cycles increases considerably to 48 in the West and to 46 in the East side.

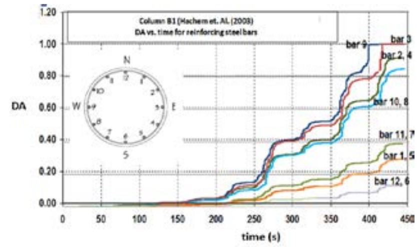

Fig. 19 – DA vs. time for reinforcing bars of UCB Column [4]

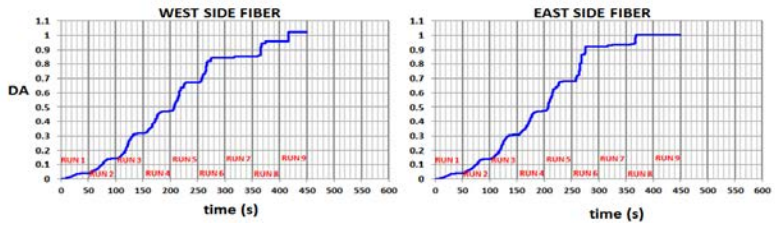

Fig. 20 - DA vs. time results in the confined concrete with the proposed new spacing of 1.8cm.

12. Conclusions

Testing of two columns, under several earthquakes, studied here, demonstrated that the code provide excellent methods for seismic design of reinforced concrete bridge columns for the specified life-safety earthquake. However, in areas of high seismic hazard, several earthquakes of different intensities may excite the column and the responses will contain a number of reversal strains inducing DA in the materials therefore, it becomes important to study seismic response including DA and LCF.

To meet PBSD several records should be used and every one induces an amount of damage that can be captured by DA and LCF models however, at present, codes do not require to accumulate damage on a structure during every earthquake. DA required calibrations of *m*, Eq. (1), for each column, and calibrated values are similar thus, if more columns are studied a reliable value of *m* will permit to predict, during design, the occurrence of the first failure that for the columns was crushing of the concrete, with not previous test.

The comparison of responses including previous records effects, PRE responses, which capture DA for every record, with NPRE responses which do not capture DA, show that during PRE responses failures occurred when DA reached 100% in the material fibers which are then removed by LCF model and the predictions agreed with test results. When DA is not captured, NPRE responses exhibit larger stiffness, strength, and ductility ratios capacities than PRE responses, and even none of the observed failures.

According to the code, instability at 60cm displacement controls the design of the UCSD column, and at 16cm the design of the UCB column however, according to this study crushing of the confined concrete occurred previously at 57cm and 12cm respectively. DA and LCF changed the mechanism controlling the design [19]: from instability to crushing of the confined concrete.

Regarding strains, maximum ones captured did not reach even half the maximum code specified strains [19], however failures occurred, no after those maximum but due to a number of strains captured during previous records in addition to the maximum strains captured at failures.

To prevent crushing, one proposal is presented: Reduce the code calculated spacing of the hoops or increase the corresponding bar diameter. In this study, reducing 40% the code hoops spacing, same bar diameter, will increase the maximum confined strength and the ultimate strain of the confined section [11] delaying the occurrence of crushing since the number of peak strains required to induce such failure, increases.

Based on the results for the two columns, which characteristics are similar, subduction earthquakes require more reversals strains but with lower amplitudes than earthquakes containing long pulses to cause failure. Another fact is that fracture of bars requires a larger number of inelastic strains, at least 95 for first fracture, than peak compression strains, about 12, required to induce crushing of the confined concrete.

Stiffness degradation in the concrete induced by DA, does not cause strength reduction at maximum displacement demand, [23]. However, strength reduces at maximum response demand when, in addition to stiffness degradation, bars fracture due to LCF.

13. References

[1] American Society of Civil Engineers (2007): Seismic Rehabilitation of Existing Buildings ASCE/SEI 41-07.
[2] Federal Emergency Management Agency (1997): NEHRP Guidelines for the seismic rehabilitation of buildings, FEMA 273.
[3] Federal Emergency Management Agency (1997): Prestandard and Commentary for the Seismic Rehabilitation of Buildings, FEMA 356.
[4] Lara, O. (2011). "The flexural seismic resistant design of reinforced concrete bridge columns". Ph.D. Thesis, University of British Columbia, Vancouver, Canada.
[5] McKenna Frank. 1997. "Object-Oriented Finite Element Programming: Frameworks for Analysis. Algorithms and Parallel Computing". PhD Thesis, University of California, Berkeley, CA.
[6] Mazzoni, S., McKenna, F., Fenves G. L. and et al. 2006. "Open System for Earthquake Engineering Simulation User Manual". *www.opensees.berkeley.edu*.
[7] Lara, O., Ventura, C.E., and Suarez, V.A. (2010). Prediction spread sheet submitted for the "Concrete Column Blind Prediction Contest 2010" sponsored by PEER and NEES.
[8] Shoettler, M., Restrepo, J., Guerrini, G., Duck, D. and Carrea, F. 2015. "A Full-Scale, Single-Column Bridge Bent Tested by Shake-Table Excitation". Report No. PEER-2015/02. Pacific Earthquake Research Center. University of California, Berkeley, CA.
[9] Hachem, M. M., Mahin, S. A., and Moehle, J. P. 2003. "Performance of Circular Concrete Bridge Columns under Bidirectional Earthquake Loading". Report No. PEER-2003/06. Pacific Earthquake Research Center. University of California, Berkeley, CA.
[10] Taucer, F., Spacone, E., and Filippou, F. C. 1991. "A fiber beam-column element for seismic response analysis of reinforced concrete structures". Report No. UBC/EERC-91/17.Earthquake Engineering Research Center. University of California, Berkeley, CA.
[11] Mander, J. B., Priestley, M. J. N., and Park, R. 1988. "Theoretical Stress-Strain Model for Confined Concrete". Journal of Structural Engineering, Vol. 114, Nº 8, ASCE.
[12] Giuffre, A. and Pinto, P.E. 1970. "Il Comportamento del Cemento Armato per Sollecitazioni Cicliche di Forte Intensità". Giornale del Genio Civile.
[13] Menegotto, M. and Pinto, P.E. 1973. "Method of Analysis for Cyclically Loaded Reinforced Concrete Plane Frames Including Changes in Geometry and Non-Elastic Behavior of Elements under Combined Normal Force and Bending".
[14] Miner, M. A. 1945."Cumulative Damage in fatigue". Journal of Applied Mechanics, Vol. 12, pages A-159.
[15] Coffin, L. F. Jr. 1954. "A study on the effects of cyclic thermal stresses on a ductile metal". Transactions of the American Society of Mechanicals Engineers. New York, N. Y., 76, pages 931-950.
[16] Manson, S. S. 1953. "Behavior of materials under conditions of thermal stress". Heat Transfer Symposium, University of Michigan Engineering Research Institute, Ann Arbor, Michigan, pages 9-75.
[17] Brown, J., Kunnath, S.K. 2004. "Low-Cycle Fatigue Behavior of Reinforcing Steel Bars". ACI Materials Journal, Vol.101, No.6, 457-466.
[18] Pacific Earthquake Engineering Research Center (PEER) and Network for Earthquake Engineering Simulation (NEES). 2010. "Concrete Column Blind Prediction Contest 2010". Column Tested at NEES Large High-Performance Outdoor Shake Table. Englekirk Structural Engineering Center. University of California, San Diego CA. http://nisee2.berkeley.edu/peer/prediction_contest/
[19] American Association of State Highway and Transportation Officials. 2007. Proposed AASHTO Guide Specifications for LRFD Seismic Bridge Design. Subcommittee for Seismic Effects on Bridges T-3. Washington, D.C.
[20] Moehle, J. 2015. Seismic Design of Reinforced Concrete Buildings 1st Edition. Mc Graw Hill Education.
[21] Lara, O. 2012. "Cumulative Damage Study for the 2010 Blind Prediction Contest of a Reinforced Concrete Bridge Column" 15 WCEEM, Lisboa, Portugal.
[22] Kunnath, S. K., El-Bahy, A., Taylor, A. W. and Stone, W. C. 1997. "Cumulative Seismic Damage of Reinforced Concrete Bridge Piers". National Institute of Standards and Technology (NIST), Report No 6075.
[23] Clough, R. W. 1966. "Effect of Stiffness Degradation on Earthquake Ductility Requirements". UCB/SESM-1966/16, Dept. of Civil Engineering, University of California, Berkeley.